Optics Communications 380 (2016) 21–27

Contents lists available at ScienceDirect

Optics Communications

journal homepage: www.elsevier.com/locate/optcom

# Image enhancement by spatial frequency post-processing of images obtained with pupil filters

Irene Estévez [a], Juan C. Escalera [a], Quimey Pears Stefano [b], Claudio Iemmi [b], Silvia Ledesma [b], María J. Yzuel [a], Juan Campos [a,*]

[a] Departamento de Física, Universidad Autónoma de Barcelona, 08193 Bellaterra, Spain
[b] Departamento de Física, FCEyN, Universidad de Buenos Aires, Buenos Aires 1428, Argentina

ARTICLE INFO

*Article history:*
Received 10 March 2016
Received in revised form
26 May 2016
Accepted 27 May 2016

*Keywords:*
Image enhancement
Diffraction
Apodization
Resolution

ABSTRACT

The use of apodizing or superresolving filters improves the performance of an optical system in different frequency bands. This improvement can be seen as an increase in the OTF value compared to the OTF for the clear aperture.

In this paper we propose a method to enhance the contrast of an image in both its low and its high frequencies. The method is based on the generation of a synthetic Optical Transfer Function, by multiplexing the OTFs given by the use of different non-uniform transmission filters on the pupil. We propose to capture three images, one obtained with a clear pupil, one obtained with an apodizing filter that enhances the low frequencies and another one taken with a superresolving filter that improves the high frequencies. In the Fourier domain the three spectra are combined by using smoothed passband filters, and then the inverse transform is performed. We show that we can create an enhanced image better than the image obtained with the clear aperture. To evaluate the performance of the method, bar tests (sinusoidal tests) with different frequency content are used. The results show that a contrast improvement in the high and low frequencies is obtained.



## 1. Introduction

There are different image quality criteria to analyse the image performance of an optical system. The Point Spread Function (PSF) is commonly used to that purpose [1,2]. The Optical Transfer Function (OTF) and the Modulation Transfer Function are used to analyse the frequency transmission of an optical system [3–6] with incoherent illumination.

Pupil filters have been widely used to improve some characteristics of the response of optical systems [7–10]. For instance, apodizing filters can reduce secondary maxima on the PSF [11]. Different types of superresolving filters have been used to sharpen the principal maximum of the PSF, increasing the resolving power [12,13].

Sheppard and Hegedus [14] introduced some performance parameters that describe the focusing properties of rotationally-symmetric pupil filters or masks in the paraxial regime. These factors are expressed simply in terms of the moments of the pupil, and avoid the necessity to calculate the diffracted field of the lens. These gains were generalized in [15] for phase filters, working also near the paraxial plane. Nevertheless, a complex pupil filter can shift the Best Image Plane (BIP) away from the best image plane without filter. So, in [16] we generalized the gain parameters for any complex filter in the surroundings of the shifted focus.

In the last years many papers deal with the fast-developing area of computational photography where a combination of imaging techniques and efficient image processing algorithms are done to generate a super imaging system. Three main implementations of the computational photography philosophy have been intensively investigated and demonstrated: (i) multiple aperture, (ii) light field photography, and (iii) multiexposure [17–20].

In this paper we investigate an enhancement method of the third kind (multiexposure). We show that the OTF produced by some apodizing filters is better than clear pupil for low frequencies, though the transmission of high frequencies is worst. On the contrary, we also show that some superresolving filters transmit better the high frequencies than the clear pupil, but with bad behavior in the low frequency spectrum. So, we propose to capture an image obtained with the low pass filter (apodizing filter) and another taken with the high pass filter (superresolving filter). Then, we combine the low and high frequency content from both images through a post-processing. We show that we can create an enhanced image better than the obtained with the clear

* Corresponding author.
*E-mail address:* juan.campos@uab.es (J. Campos).

http://dx.doi.org/10.1016/j.optcom.2016.05.076
0030-4018/

aperture. Special care has to be taken in how the frequency multiplexing is done, to avoid unwanted effects on the global response. To check the effect of this process in an image, bar tests (sinusoidal tests) with different frequency content are used.

The process can be summarized as follows. Firstly, we calculate the Modulation Transfer Function (MTF) of the clear pupil and those produced by the apodizing and superresolving filter. Then, we compare the three MTFs and we decide which part of the spectrum is better for each pupil. Secondly, we select the best annular zones of the Fourier spectrum of each pupil, and we multiplex them. Thirdly, an inverse Fourier transform is calculated, obtaining the enhanced image. The whole process is also applied to the images of sinusoidal bar tests. The frequency content of the enhanced and the original images are compared to analyse the goodness of the procedure.

In Section 2 we study different pupil designs that can produce a suitable apodizing or superresolving response. On one side we study amplitude filters, polynomial (Section 2.1) or supergaussian ring filters (Section 2.2). Once we have chosen the suitable pupil filters (apodizing and superresolving) (Section 2.3) we calculate the MTFs for each pupil. In Section 3 we describe in a detailed way the spatial frequency post-processing method we propose to merge the MTFs of the images obtained with the clear pupil, the apodizing filter and the superresolving filter. In Section 4 we show the enhanced images with extended object obtained with the different designs. Finally, in Section 5, we expose our conclusions.

## 2. Pupil design

In this section we analyse different pupil designs that produce apodizing and superresolving filters suitable for this application.

### 2.1. Pupil design: polynomial amplitude filters

First, we are going to look for polynomial amplitude filters that can produce apodization or superresolution in the focal plane. Polynomial amplitude filters have been widely used to produce either apodization or superresolution. For instance, we showed in [21] that filter with transmission amplitude $P(r)=1-r^2$ produces apodization in the focal plane, and that filter $P(r)=r^2$ produces superresolution in that plane. If we calculate the performance parameters proposed by Sheppard and Hegedus [14], we obtain the results we show in Table 1. Both filters produce the same axial gain, Strehl ratio and transmitted energy, in fact we showed in [21] that they produce the same axial response. Nevertheless, in the best image plane filter $P(r)=1-r^2$ is an apodizing filter (transverse gain is lower than 1) and filter $P(r)=r^2$ is superresolving (transverse gain is higher than 1).

In Fig. 1 we show the MTFs produced by the clear pupil, the apodizing and the superresolving polynomial filters. In Fig. 1 the cut-off frequency for the clear pupil has been normalized to one. We see that the apodizing filter ($P(r)=1-r^2$) is better in the low frequency region, the clear aperture in the mid frequency region and the superresolving filter ($P(r)=r^2$) in the high frequency region. So, we see that these polynomial filters are suitable for the intended application.

**Table 1**
Performance parameters on the best image plane for the filters: filter 1, $P(r)=r^2$; filter 2, $P(r)=1-r^2$.

| Pupil filter | Transverse gain ($G_T$) | Axial gain ($G_A$) | Strehl ratio (S) | Transmitted energy (E) | $F=S/E$ |
|---|---|---|---|---|---|
| **Filter 1: $P(r)=r^2$** | 4/3 | 2/3 | 1/4 | 1/3 | 3/4 |
| **Filter 2: $P(r)=1-r^2$** | 2/3 | 2/3 | 1/4 | 1/3 | 3/4 |

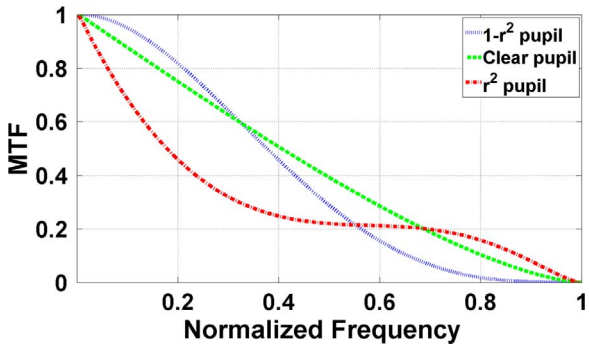


**Fig. 1.** Modulation Transfer Function (MTF) obtained with a) $1-r^2$ filter, pupil 1 (dotted line) b) Clear pupil, pupil 2 (dashed line), c) $r^2$ filter, pupil 3 (dashed dotted line).

### 2.2. Pupil design: supergaussian ring amplitude filters

The purpose of this section is to investigate supergaussian ring amplitude filters that can be tuned to obtain a specific MTF (apodizing or superresolving response). Moreover, we intend to improve other parameters of the optical response. In particular, it is of interest to find amplitude filters that have a good performance in PSF and MTF response, but with good transmitted energy and Strehl ratio, in order to improve their practical implementation.

In [22] the use of supergaussian rings (SGR) was proposed. In a later work [23], we studied general conditions that complex and real valued pupil filters must satisfy to produce identical axial response. When we looked for practical examples, we realized that it was better to modify the supergaussian rings in the variable $r$ (radial coordinate in the pupil plane) to supergaussian rings in variable $t=r^2$:

$$Q(t) = \exp\left\{ -\left[ (t - t_0)/\Omega \right]^{2\alpha} \right\} \tag{1}$$

These pupil functions depend on three parameters. The parameter α determines the shape of the filter, for $\alpha=1$ the amplitude transmittance becomes an annular Gaussian ring, and for $\alpha \to \infty$ the supergaussian ring is identical with an annular aperture or a ring window. For practical applications we can consider that for $\alpha \geq 5$ the supergaussian ring can be approximated to a ring window. The parameter $\Omega$ controls the width of the ring. $\alpha$ and $\Omega$ can modify the value of the transmitted energy ($E$) of the pupil, especially $\Omega$. Finally, $t_0$ is the center of the supergaussian profile (in the variable $t=r^2$) and if the supergaussian ring is not truncated appreciably in the interval [0, 1], the pupil function is symmetrical and then the value of $t_0$ coincides with the centre of gravity of the pupil transmission and the transversal gain is $G_T=2t_0$.

We have done an extensive study of the supergaussian rings suitable for this application. First we have calculated the parameters $G_A$, $S$, $E$ and $F$ defined in [14] for supergaussian rings in t for different values of the SG ring parameters $\alpha$, $\Omega$ and $t_0$. The supergaussian rings suitable for being apodizing must have $\alpha=1$ in order to have a soft shape (not abrupt) and the best results (in terms of apodization) are obtained for $t_0=0$. Then, we vary the parameter $\Omega$. Some of these results are shown in Table 2. We see that all of them are apodizing, since $G_T$ is lower than 1, but in some cases the Strehl ratio and the transmitted energy is very low.

**Table 2**
Supergaussian rings in $t$, $\alpha=1$, $t_0=0$ and different values of $\Omega$.

| $\Omega$ | Transverse gain ($G_T$) | Axial gain ($G_A$) | Strehl ratio ($S$) | Transmitted energy (E) | $F=S/E$ |
|---|---|---|---|---|---|
| **0.2** | 0.225 | 0.087 | 0.031 | 0.125 | 0.250 |
| **0.4** | 0.450 | 0.345 | 0.125 | 0.250 | 0.500 |
| **0.6** | 0.646 | 0.647 | 0.272 | 0.375 | 0.725 |
| **0.8** | 0.773 | 0.816 | 0.428 | 0.495 | 0.864 |
| **1.0** | 0.846 | 0.895 | 0.557 | 0.598 | 0.932 |

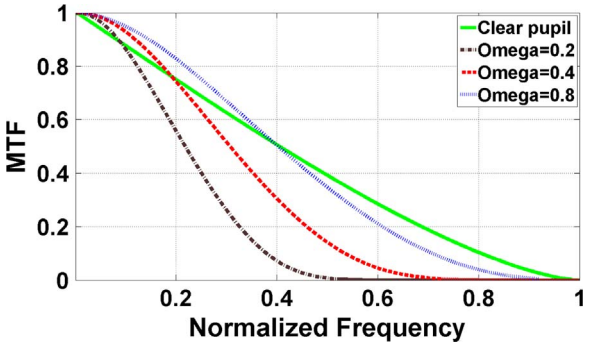


**Fig. 2.** Modulation transfer function (MTF) produced by the: (a) clear pupil (solid line); apodizing supergaussian rings with $t_0=0$, $\alpha=1$ and: (b) $\Omega=0.2$ (dashed dotted line), (c) $\Omega=0.4$ (broken line) and (d) $\Omega=0.8$ (dotted line).

Finally, we choose three designs of apodizing supergaussian rings, with the following parameters: $t_0=0$, $\alpha=1$, and $\Omega=0.2$, 0.4 and 0.8. In Fig. 2 we show the three MTFs produced by these filters in comparison to the MTF of the clear pupil. It is clear that the MTF produced by the supergaussian ring with parameters $t_0=0$, $\alpha=1$, and $\Omega=0.8$ is the best. It has an extended zone in the low frequency region with higher values than the clear pupil. We see that this filter has a Strehl ratio of about 0.5 what leads to a good compromise between a low transverse gain and a minimum Strehl ratio. It is also very interesting to remark that this apodizing SGR ($\Omega=0.8$) has much better transmitted energy (0.495 versus 0.33) and Strehl ratio (0.428 versus 0.25) that the polynomial apodizing filter (see Tables 1 and 2). On the other hand if Figs. 1 and 2 are compared it can be seen that they produce a very similar frequency enhancement on the low frequency region that we will study with more detail in Section 3.

In a similar way we analyse the response of superresolving supergaussiang rings. Starting from $\alpha=1$ in order to have a soft shape (not abrupt) and $t_0=0.9$ for obtaining the best results in terms of superresolution $\Omega$ is varied. Some of these results are shown in Table 3. Although all of them are superresolving, since $G_T$ is higher than 1, in some cases for obtaining the best results in terms of superresolution Strehl ratio and the transmitted energy is very low, therefore it is necessary to compare the MTFs to evaluate which design is better to achieve an image improvement. We will have to compare the MTFs to evaluate which design is better to enhance the image.

As an example we show in Fig. 3 the MTFs produced by the

**Table 3**
Supergaussian rings in $t$, $\alpha=1$, $t_0=0.9$ and different values of $\Omega$.

| $\Omega$ | Transverse gain ($G_T$) | Axial gain ($G_A$) | Strehl ratio ($S$) | Transmitted energy ($E$) | $F=S/E$ |
|---|---|---|---|---|---|
| **0.2** | 1.684 | 0.130 | 0.072 | 0.210 | 0.344 |
| **0.4** | 1.469 | 0.420 | 0.204 | 0.346 | 0.589 |
| **0.6** | 1.290 | 0.704 | 0.375 | 0.473 | 0.793 |
| **0.8** | 1.183 | 0.845 | 0.531 | 0.588 | 0.904 |
| **1.0** | 1.123 | 0.909 | 0.649 | 0.680 | 0.953 |

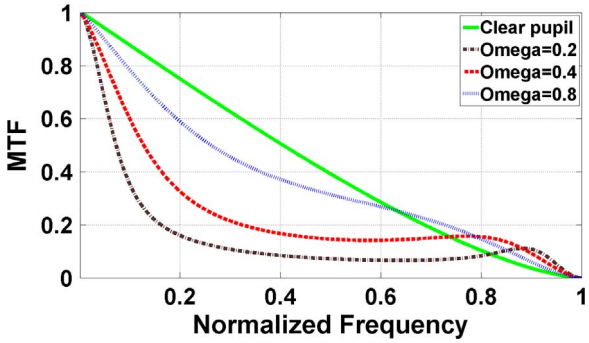


**Fig. 3.** Modulation transfer function (MTF) produced by the: (a) clear pupil (solid line); apodizing supergaussian rings with $t_0=0.9$, $\alpha=1$ and: (b) $\Omega=0.2$ (dashed dotted line), (c) $\Omega=0.4$ (broken line) and (d) $\Omega=0.8$ (dotted line).

clear pupil and by three superresolving supergaussian rings with parameters: $t_0=0.9$, $\alpha=1$, and 0.2, 0.4 and 0.80. It can be appreciated that the three supergaussian filters have a better response in the high frequency region than the clear pupil. In particular, the filter with parameters $t_0=0$, $\alpha=1$, and $\Omega=0.80$ produces a higher response over more extended zone in that region. It should be noted that this superresolving SGR ($\Omega=0.8$) has much better transmitted energy (0.588 versus 0.33) and Strehl ratio (0.531 versus 0.25) that the polynomial superresolving filter (see Tables 1 and 3). As both filters produce a very similar frequency enhancement on the high frequency region, the SGR filter is the best option for our purpose.

### 2.3. Pupil design: final selection

In the previous sections we have analysed different types of pupil filters that can be used as apodizing or superresolving filters. In Fig. 4 we show the amplitude transmission functions of the designs we have chosen, two polynomial functions and two supergaussian rings.

The two apodizing pupil functions are very similar, with maximum transmission in the centre of the pupil and a soft decay up to the outer part of the pupil. The supergaussian ring has higher transmission on the outer part of the pupil. Therefore, that makes that the total transmitted energy is higher for the apodizing SGR pupil filter.

On the other hand, the superresolving filters have high transmittance in the outer part of the pupil and lower on the inner region, with a soft decay to avoid producing ringing in the PSF. We see that the superresolving SGR has higher transmission than the filter $P(r)=1-r^2$, explaining the higher transmitted energy and Strehl ratio of the SGR filter.

So, we have selected two apodizing filters and two

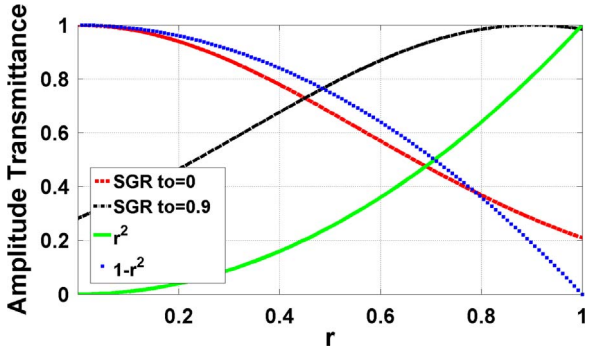


**Fig. 4.** Amplitude transmittance of the filters: a) Filter $1-r^2$ (dotted line), b) The apodizing supergaussian ring (broken line), c) Filter $r^2$ (solid line) and d) The superresolving supergaussian ring (dashed dotted line).

superresolving filters. All of them are amplitude transmission filters, meaning that they will produce a loss of energy. All of them have a good performance in PSF and MTF response, but the supergaussian ring filters are more flexible, letting us to increase the transmitted energy and Strehl ratio, in order to improve their practical implementation.

## 3. Spatial frequency post-processing method

This section presents the methodology followed in this work. First the MTFs of the three different pupils: apodizing filter (pupil 1), clear pupil (pupil 2) and superresolving filter (pupil 3) are calculated. Each of these functions is higher than the others in some frequency band. For instance, the apodizing filter (pupil 1) is better in the low frequency region; the clear aperture (pupil 2) in the mid frequency region and the superresolving filter (pupil 3) in the high frequency region.

Fig. 1, for instance, shows a graph with the three studied Modulation Transfer Functions, where we can see the different sections in which one pupil provides significantly better results than the others. The purpose of this work is to create a synthetic transfer function by combining the three previous ones. In the case of three filters, three annular frequency bands are selected to have the best transfer function. This combination takes the higher values of the MTFs for each region. The combination of the three MTFs is shown in Fig. 8 with continuous line. To avoid the abrupt junctions at the intersection points of the MTFs ($f_1$ and $f_2$), a linear combination of the two adjacent MTFs is taken. In this way the unions are soften. Let $\tilde{O}(f)$ be the Fourier Transform of the input object, and $\tilde{i}_1(f) = \tilde{O}(f)*OTF_1(f)$, $\tilde{i}_2(f) = \tilde{O}(f)*OTF_2(f)$ and $\tilde{i}_3(f) = \tilde{O}(f)*OTF_3(f)$ be the Fourier Transform of the images obtained with pupil 1, pupil 2 and pupil 3 respectively. From these Fourier Transforms we generate a combined (enhanced) Fourier Transform $\tilde{i}(f)$.

Fig. 5 shows how we divide the Fourier domain in five regions. The first region goes from 0 up to $a_1$, in this región $\tilde{i}(f) = \tilde{i}_1(f)$. The second region goes from $a_1$ to $b_1$ and in this band frequency region $\tilde{i}(f)$ is evaluated by the following expression:

$$\tilde{i}(f) = \tilde{O}(f)\left( OTF_1(f)\frac{f-b_1}{a_1-b_1} + OTF_2(f)\frac{f-a_1}{b_1-a_1}\right) = \tilde{i}_1(f)\frac{f-b_1}{a_1-b_1} + \tilde{i}_2(f)\frac{f-a_1}{b_1-a_1} \quad (2)$$

where $OTF_1$ and $OTF_2$ are the Optical Transfer Functions of the pupils 1 and 2, $a_1$ and $b_1$ are the first and last points of the interval where we try to smooth the transition and f is the frequency. The third region goes from $b_1$ up to $a_2$, in this región $\tilde{i}(f) = \tilde{i}_2(f)$. The fourth region goes from $a_2$ to $b_2$. In this region $\tilde{i}(f)$ is evaluated in a similar way as we have described in Eq. (1) but in this case with the OTFs corresponding to pupils 2 and 3. The fifth region goes from $b_2$ to the cut-off frequency. In this region we take $\tilde{i}(f) = \tilde{i}_3(f)$.

In general, pupil filters may produce different transmitted

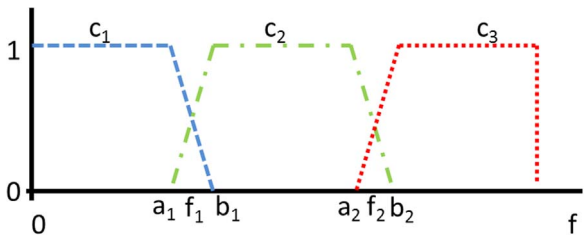


**Fig. 5.** Distribution of the five regions in the Fourier domain.

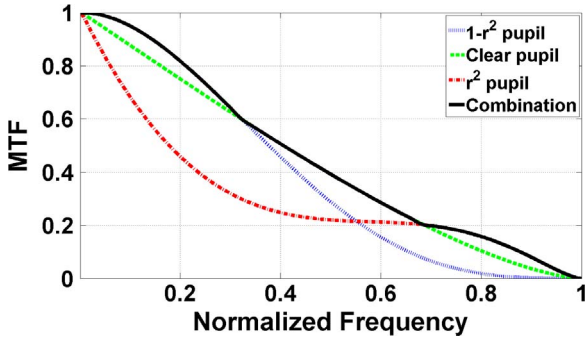


**Fig. 6.** Modulation Transfer Function (MTF) obtained with: a) $1-r^2$ filter, pupil 1 (dotted line) b) Clear pupil, pupil 2 (dashed line), c) $r^2$ filter, pupil 3 (dashed dotted line) d) Combination (solid line).

energy. Then, some coefficients are needed for the filters in order to normalize the MTFs to produce the same maximum value.

Finally, by calculating the inverse Fourier transform of the multiplexed information in the Fourier domain $\tilde{i}(f)$, the optimized image is obtained.

Fig. 6 shows the MTFs produced with the polynomial amplitude filters we studied in Section 2.1: the apodizing filter is the filter $(1-r^2)$ and the superresolving filter is the filter $(r^2)$. In solid line is also shown the enhanced MTF function obtained combining the MTFs of the apodizing, clear pupil and superresolving filter.

In Fig. 7 we show the MTFs produced by the clear pupil and the apodizing and superresolving supergaussian ring filters we selected in Section 2.2. We see that the apodizing filter ($t_0=0$, $\alpha=1$, $\Omega=0.8$) is better in the low frequency region; the clear aperture in the mid frequency region and the superresolving filter ($t_0=0.9$, $\alpha=1$, $\Omega=0.8$) in the high frequency region. With continuous line we show the combined MTF that we propose to improve the spatial frequency response.

Fig. 8 shows a comparison of the MTFs produced by the clear pupil and both the polynomial and supergaussian ring apodizing and superresolving filters. First, we compare the low frequency region. The MTF is better for the filter $1-r^2$ for very low frequencies (Fig. 9). As the frequency increases, the MTF for the filter $1-r^2$ decays faster than for the apodizing supergaussian filter, being the second one better.

Secondly, we analyse the high frequency region. At very high frequencies, the MTF produced by the filter $r^2$ is the highest, but for lower range of frequencies, the MTF produced by the superresolving supergaussian ring is better. For the intermediate range of frequencies the best results are obtained with the clear pupil.

Note that the results we show are an example of the technique. In this work, we have used filters to improve the contrast in the low and high frequency zones, but we can divide the pupil in more

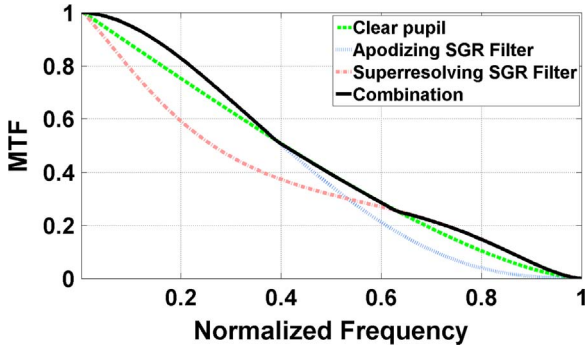


**Fig. 7.** MTF produced by the: (a) apodizing supergaussian ring (dotted line), (b) clear pupil (dashed line), (c) superresolving supergaussian ring (dashed dotted line) and (d) combination (solid line).

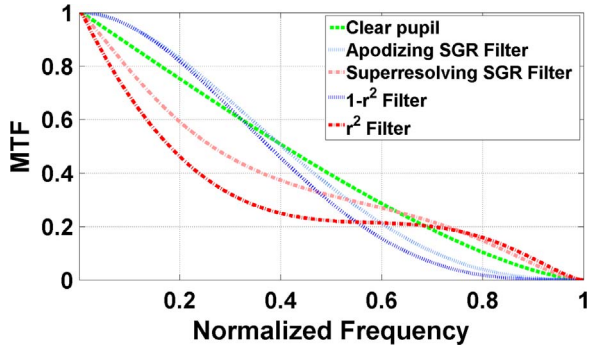


**Fig. 8.** MTF obtained with the: a) Clear pupil (broken line), b) Apodizing supergaussian ring (light dotted line), c) Filter $1-r^2$ (dark dotted line), d) Superresolving supergaussian ring (light dashed dotted line), e) Filter $r^2$ (dark dashed dotted line).

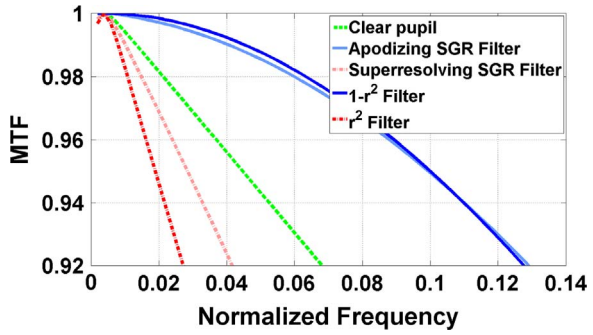


**Fig. 9.** Zoom of the low frequency region of the MTF obtained with the: a) Clear pupil (broken line), b) Apodizing supergaussian ring (light blue line), c) Superresolving supergaussian ring (light dashed dotted line), d) Filter $r^2$ (dark dashed dotted line), and e) Filter $1-r^2$ (dark blue line). (For interpretation of the references to color in this figure legend, the reader is referred to the web version of this article.)

frequency bands and use the filters that increase the contrast in these regions. On the other hand, if one increases the number of filters, the time to take the image also increases as well as the artefacts that can create the transitions between zone filters. Therefore, we have to make a trade-off between the contrast improvement and the time to take the images and process them.

## 4. Enhanced images obtained with extended objects

In this section we analyse the simulation results obtained with extended objects. The extended image study is performed by using a sinusoidal bars test with variable frequency is generated to have an object with the frequencies well localized in the spatial domain. This frequency test corresponds to the function:

$$T = \frac{1}{2}\left[1 + \sin 2\pi\nu(x)\cdot x\right] \tag{3}$$

where $\nu$ is a variable that linearly increases to obtain all the frequencies. This is shown in Fig. 10(a and b). As the object is quite long, we have selected two zones of interest: the high frequency region (Fig. 10a) and the low frequency region (Fig. 10b). So, each image is divided in two parts, the zoom of the high frequencies on the top and the low frequency region on the bottom.

The image obtained by the clear pupil (Fig. 10(c and d)) shows a decrease on the contrast for all the frequencies, especially for the high ones (Fig. 10(c)). On the left zone of Fig. 10(c) we can see the frequencies that are close to the diffraction limit, that are not transmitted by the clear pupil.

Fig. 11 shows the image obtained with the apodizing and superresolving polynomial filters. These images can be compared

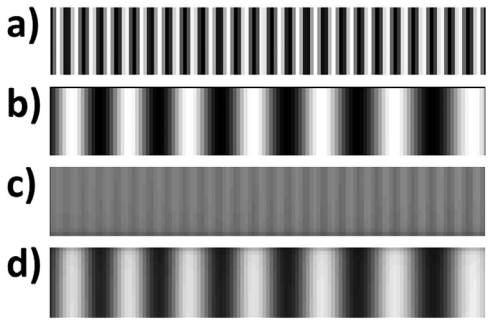


**Fig. 10.** Sinusoidal bar test, zoom of the: (a) high frequency region and (b) low frequency region. image obtained with the clear pupil, zoom of the: (c) high frequency region and (d) low frequency region.

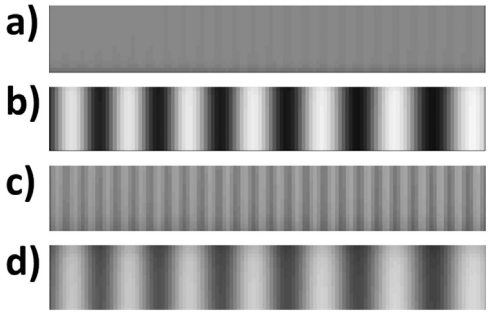


**Fig. 11.** Image obtained with the $1-r^2$ filter, zoom of the: (a) High frequency region and (b) Low frequency region. Image obtained with the $r^2$ filter, zoom of the: (c) High frequency region and (d) Low frequency region.

with the image produced by the clear pupil (Fig. 10(c and d)). The image obtained with the $1-r^2$ filter shows a contrast decrease in the high frequency band filter (Fig. 11(a)) and an increase of the contrast on the low band filter (Fig. 11(b)). The contrary happens by using the $r^2$ filter, it shows a contrast increase in the high frequency band filter (Fig. 11(c)) and a decrease of the contrast on the low band filter (Fig. 11(d)).

Fig. 12 shows the image obtained with the apodizing and superresolving supergaussian ring filters. These images can be compared with the image produced by the clear pupil (Fig. 10) and also with the corresponding images obtained with the polynomial filters (Fig. 11). The image obtained with the SGR apodizing filter shows a contrast decrease in the high frequency band filter (Fig. 12 (a)) and an increase of the contrast on the low band filter (Fig. 12 (b)). The contrary happens by using the SGR superresolving filter, it shows a contrast increase in the high frequency band filter (Fig. 12(c)) and a decrease of the contrast on the low band filter (Fig. 12(d)).

Finally, in Fig. 13 we compare the enhanced images of the bar

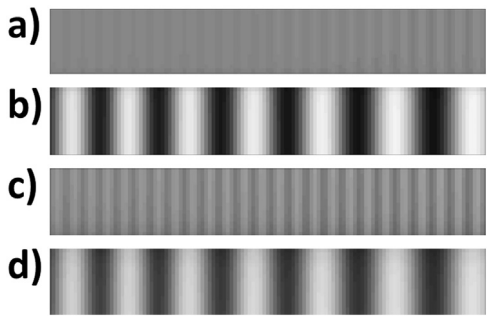


**Fig. 12.** Image obtained with the supergaussian apodizing filter, zoom of the: (a) high frequency region and (b) low frequency region. image obtained with the supergaussian superresolving filter, zoom of the: (c) high frequency region and (d) low frequency region.

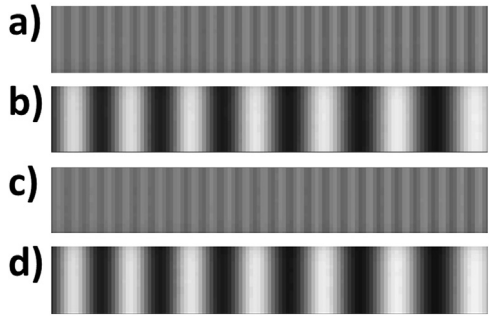


**Fig. 13.** Enhanced images obtained by: The polynomial filters, zoom of the: (a) high frequency region and (b) low frequency region; the supergaussian filters, zoom of the: (c) high frequency region and (d) low frequency region.

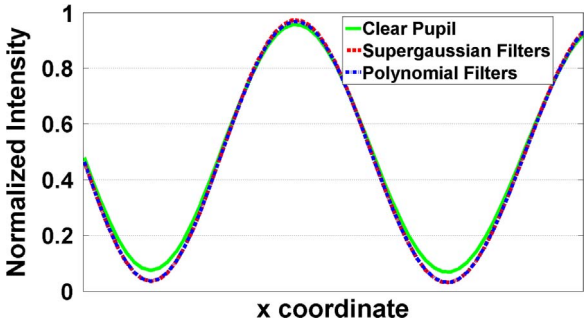


**Fig. 14.** Profile line graphs in the low frequency region obtained with the: A) clear pupil (solid line), b) supergaussian filters (broken line), polynomial filters (dashed dotted line). (For interpretation of the references to color in this figure legend, the reader is referred to the web version of this article.)

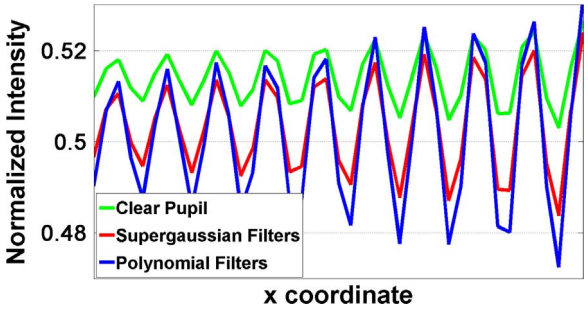


**Fig. 15.** Profile line graphs in the high frequency region obtained with the: a) clear pupil (solid green line), b) supergaussian filters (solid red line), polynomial filters (solid blue line). (For interpretation of the references to color in this figure legend, the reader is referred to the web version of this article.)

test obtained with the combination of the polynomial filters and clear pupil (Fig. 13(a and b)) and the enhanced image obtained with the combination of the supergaussian ring filters and clear pupil (Fig. 13(c), (d)). Both the polynomial enhanced image (Fig. 13 (a)) and the supergaussian enhanced image (Fig. 13(c)) are better in the high frequency region than the clear pupil image (Fig. 10(c)). On the low frequency region the best results are obtained by the polynomial filters (Fig. 13(b)), then the supergaussian filters (Fig. 13(d)), being both better than the clear pupil (Fig. 10(d)).

Comparing the enhanced images, it seems that the polynomial filters produce a higher contrast on the very high frequencies (Fig. 13(a)). On the other side, the main advantage of using the supergaussian filters is that they transmit more energy, it would permit to obtain brighter experimental images.

In order to summarize the results and quantify the improvement of the processed images, line profiles corresponding to the low frequency region, are shown in Fig. 14. It can be seen that the responses produced by the supergaussian a polynomial filters are almost the same, and in both cases with better contrast than the clear pupil.

Fig. 15 shows line profiles of images corresponding to the high frequency region. In this case it can be seen that the image produced by the clear pupil exhibits a very low contrast. On the contrary, the two enhanced images show a contrast improvement, being a little better that given by the polynomial filters. These figures clearly show the enhancement on the image produced by the spatial frequency post-processing method we propose.

## 5. Conclusions

A method to improve the contrast in low and high frequency bands of an imaging system is proposed. It is based on the generation of a synthetic Optical Transfer Function, by multiplexing the OTFs given by the use of different non-uniform transmission filters on the pupil.

The use of different types of pupil filters is investigated. Amplitude filters are shown to be suitable, in particular we have considered some types of polynomial and supergaussian ring filters. Two examples are given by using the clear aperture, an apodizing filter that improves the low frequencies, and a superresolving filter that improves the high frequencies. We have shown that the supergaussian ring filters can produce similar results to the polynomial amplitude filters but with much better transmission of light.

The final image is obtained in the Fourier domain by performing a combination of the three spectra. The transition between bands is smoothed to avoid artifacts on the final image that is obtained by inverse Fourier transforming the combined spectrum. The numerical simulations with an extended object show that a contrast improvement in all frequencies is obtained.

## Acknowledgments

This work has been funded by Ministerio de Economía y Competitividad and FEDER funds (FIS2015-66328-C3-1-R) and the Generalitat de Catalunya contract SGR2014-1639. I. Estévez also acknowledges financial support from FPI Grant no. BES-2013-064046 funded by Ministerio de Economía y Competitividad (Spain). C. Iemmi, S. Ledesma and Q. Pears Stefano appreciates the support from UBACyT 20020100100727BA and ANPCYT PICT 2014-02432 (Argentina).

## References

[1] M.J. Yzuel, F. Calvo, Opt. Acta 30 (1983) 233.
[2] H.F.A. Tschunko, Appl. Opt. 22 (1983) 133.
[3] B.R. Frieden, J. Opt. Soc. Am. 57 (1967) 56.
[4] C.J.R. Sheppard, Optik 72 (1986) 131.
[5] R. Hild, J. Campos, M.J. Yzuel, C. Iemmi, R. Gimeno, J.C. Escalera, Proc. SPIE 7000 (2008) 700018.
[6] P.W. Nugent, J.A. Shaw, Opt. Eng. 49 (2010) 103201.
[7] H. Wang, C.J.R. Sheppard, K. Ravi, S.T. Ho, G. Vienne, Laser Photonics Rev. (2011) 1.
[8] S. Ledesma, J.C. Escalera, J. Campos, M.J. Yzuel, Opt. Commun. 249 (2005) 183.
[9] C.J.R. Sheppard, J. Campos, J.C. Escalera, S. Ledesma, Opt. Comm. 281 (2008) 913.
[10] C.J.R. Sheppard, J. Campos, J.C. Escalera, S. Ledesma, Opt. Comm. 281 (2008) 3623.
[11] J.E. Wilkins Jr, J. Opt. Soc. Am. 67 (1977) 1027.
[12] J. Ojeda-Castañeda, C.M. Gómez-Sarabia, Adv. Opt. Photonics 7 (2015) 814.
[13] C.J.R. Sheppard, A. Choudhury, Appl. Opt. 43 (2004) 4322.
[14] C.J.R. Sheppard, Z.S. Hegedus, J. Opt. Soc. Am. A 5 (1988) 643.
[15] D.M. de Juana, J.E. Oti, V.F. Canales, M.P. Cagigal, Opt. Lett. 28 (2003) 607.
[16] S. Ledesma, J. Campos, J.C. Escalera, M.J. Yzuel, Opt. Lett. 29 (2004) 932.
[17] D. Mendlovic, Appl. Opt. 52 (2013) 561.

[18] A. Kanaev, J. Ackerman, E. Fleet, D. Scribner, Opt. Lett. 32 (2007) 2855.
[19] M. Robinson, D. Stork, Appl. Opt. 47 (2008) B11.
[20] J. Ojeda-Castañeda, E. Yepez-Vidal, C.M. Gómez-Sarabia, Appl. Opt. 52 (2013) D84.
[21] M.J. Yzuel, J.C. Escalera, J. Campos, Appl. Opt. 29 (1990) 1631.
[22] J. Ojeda-Castañeda, J.C. Escalera, M.J. Yzuel, Opt. Comm. 114 (1994) 189.
[23] J. Campos, J.C. Escalera, C.J.R. Sheppard, M.J. Yzuel, J. Mod. Opt. 47 (2000) 57.